

# Compact Early Vision Signal Analyzers in Neuromorphic Technology

**Conference Paper****Author(s):**

Baruzzi, Valentina; Indiveri, Giacomo ; Sabatini, Silvio P.

**Publication date:**

2020-01-01

**Permanent link:**

<https://doi.org/10.3929/ethz-b-000447622>



**Rights / license:**

[Creative Commons Attribution-NonCommercial-NoDerivatives 4.0 International](#)

**Originally published in:**

4, <https://doi.org/10.5220/0009171205300537>

# Compact Early Vision Signal Analyzers in Neuromorphic Technology

Valentina Baruzzi<sup>1</sup>, Giacomo Indiveri<sup>2</sup><sup>a</sup> and Silvio P. Sabatini<sup>1</sup><sup>b</sup>

<sup>1</sup>*Department of Informatics, Bioengineering, Robotics and Systems Engineering, University of Genoa, Genoa, Italy*

<sup>2</sup>*Institute of Neuroinformatics, University of Zürich and ETH Zürich, Zürich, Switzerland*


**Keywords:** Early Vision, Gabor Filters, Receptive Fields, Neuromorphic Engineering, Event-based Sensors, Bioinspired Vision, Harmonic Representations.

**Abstract:** Reproducing the dynamics of biological neural systems using mixed signal analog/digital neuromorphic circuits makes these systems ideal platforms to implement low-power bio-inspired devices for a wide range of application domains. Despite these principled assets, neuromorphic system design has to cope with the limited resources presently available on hardware. Here, different spiking networks were designed, tested in simulation, and implemented on the neuromorphic processor DYNAP-SE, to obtain silicon neurons that are tuned to visual stimuli oriented at specific angles and with specific spatial frequencies, provided by the event camera DVS. Recurrent clustered inhibition was successfully tested on spiking neural networks, both in simulation and on the DYNAP-SE board, to obtain neurons with highly structured Gabor-like receptive fields (RFs); these neurons are characterized by tuning curves that are sharper or at least comparable to the ones obtained using equivalent feed-forward schemes, but require a significantly lower number of synapses. The resulting harmonic signal description provided by the proposed neuromorphic circuit could be potentially used for a complete characterization of the 2D local structure of the visual signal in terms of phase relationships from all the available oriented channels.

## 1 INTRODUCTION

The goal of early vision is to extract as much information as possible about the structural properties of the visual signal. Such a process must be efficient, providing reliable features of high informative content in short time, in order not to compromise the efficacy of subsequent processing stages, and without being, at the same time, an unbearable bottleneck. Recent asynchronous event-driven cameras combined with brain-inspired spiking neuromorphic processors can be a solution. They, indeed, constitute reconfigurable systems of silicon neurons that operate on mixed (analog/digital) signal to achieve sophisticated real-time visual processing. Due to the implementation limit for connectivity patterns between silicon neurons, vision front-ends typically restrict themselves to be image edge and moving object detectors. Sometimes, neurons operate exclusively on temporal contrast events, disregarding the spatial contrast, that is the local spatial structure of the visual signal, obtained by integrating visual events over spatial neigh-

borhoods (e.g., (Osswald et al., 2017)). Sometimes, they implement simple (e.g., binary) feature matching, by composing local receptors outputs through receptive fields (RFs) with minimal and simple weighting profiles (e.g., (Mügglger et al., 2017)). Specific matched operators extract informative (symbolic) elements of an image, such as points and lines, but inescapably discard part of the *signal*. A more sophisticated visual signal analysis would require highly structured RFs, e.g., with 2D wavelet-like profiles to extract local amplitude, phase, and orientation information in a given frequency sub-band (cf. linear visual cortical cell responses, see e.g. (Jones and Palmer, 1987)). In general, for many image processing tasks, it is commonly used to represent an image by oriented spatial-frequency channels in which some properties of the image are better represented than in image space. The spatio-temporal properties of the resulting harmonic components have been proved to be critically important for extracting primary early vision information. Indeed, in general, as evidenced in several studies (e.g., see (Fleet and Jepson, 1993) (Ogale and Aloimonos, 2007) (Sabatini et al., 2010)), by using harmonic patterns for matching instead of

<sup>a</sup> <https://orcid.org/0000-0002-7109-1689>


<sup>b</sup> <https://orcid.org/0000-0002-0557-7306>

image luminance measures, the resulting perception is more reliable (i.e., stable), denser and immune to lighting conditions.

Since a direct implementation of such wavelet RFs on neuromorphic hardware is hampered by the limited wiring capability between silicon neurons, designing and validating efficient architectural solutions to obtain compact visual signal analyzers with minimal resource consumption becomes a key issue. In this paper, we propose an economic way to implement spike-based early-vision detectors of oriented features in given spatial frequency bandwidths that mimic the known properties of Gabor-like simple cells RFs in the primary visual cortex (V1) (Jones and Palmer, 1987). In particular, we developed a recurrent neural network architecture based on a model of the retinocortical visual pathway to obtain neurons highly tuned to oriented visual stimuli along a specific direction and with a specific spatial frequency, with Gabor-like RFs. The computation performed by the biological retina is emulated by an asynchronous event-driven Dynamic Vision Sensor (DVS) (Lichtsteiner et al., 2008), which only indicates luminance temporal changes in the image impinging on the photodiode array. Its output feeds a neuromorphic processor (DYNAP-SE) (Moradi et al., 2018) with reconfigurable silicon neurons that comprises adaptive integrate-and fire neurons and dynamic synapses. We show how the network implemented on this device gives rise to neurons tuned to specific orientations and spatial frequencies, independent of the temporal frequency of the visual stimulus. Compared to alternative feed-forward schemes, the model proposed produces highly structured RFs of any phase symmetry with a limited number of synaptic connections, thus optimizing hardware resources. We validate the model and approach with experimental results using both synthetic and natural images.

## 2 MATERIALS AND METHODS

The system setup (see Fig. 1), consists of a DVS, representing the retinal stage, whose output is fed to a DYNAP-SE board, representing the cortical stage. The sensor is composed of pixels that respond asynchronously to relative changes in light intensity, generating a stream of ‘events’ that constitute its output. Each event encodes the timestamp at which it occurred, the position of the pixel that detects it, and its polarity (ON and OFF for positive and negative intensity changes, respectively). Sensor activity is reproduced by a population of spiking ‘virtual neurons’, implemented digitally by a FPGA module on

the DYNAP-SE board, which acts as spike generator for the physical silicon neurons on the chip. One of the chips on the DYNAP-SE board is programmed so to have a specific configuration of synaptic connections, described in the following, that gives rise to silicon neurons with well-structured Gabor-like RFs. These neurons are thus tuned on a specific orientation and spatial frequency, reproducing the computation carried out by simple cells in the primary visual cortex. The ‘membrane voltage’ of selected silicon neurons can be observed using an oscilloscope and the spiking activity of the entire chip can be monitored in real time on a computer through the CTXCTL Primer interface (aiCTX, 2018).

### 2.1 Network Scheme

In order to obtain neurons with Gabor-like RFs that act as early vision feature extractors, while dealing with the limited number of synaptic connections available on the chip, we adopted the recurrent clustered inhibition approach, described in (Sabatini, 1996). Ideally, the network is thus composed of a first population of neurons representing the retinal stage (‘retina layer’) and a second population representing the cortical stage (‘V1 layer’). Each neuron of the V1 layer receives excitatory afference from a group of neurons in an elongated region on the retina layer (feed-forward kernel) and inhibitory afference from two groups of neurons of the same layer (recurrent or feed-back kernel), in regions that are displaced orthogonally to the major axis of the feed-forward kernel (see left side of Fig. 1). For both feed-forward and recurrent contributions we adopt Gaussian weighting profiles. Each neuron with such a connectivity scheme will have an induced RF with a spatial profile described by a two-dimensional Gabor function, as a result of the combination of the feed-forward excitatory and the recurrent inhibitory contributions.

### 2.2 Simulated Network

To test the efficacy of the recurrent clustered inhibition approach for the the spiking neuron implementation, the network was first simulated by using Brian2 (Stimberg et al., 2019) and its toolbox *teili* (Milde et al., 2018). This simulator for spiking neural networks implements the model of the physical silicon neurons on the DYNAP-SE board. The simulated network has the structure described above, and discrete nature.

The use of sinusoidal gratings as visual input allowed us to extract the spatial frequency and orientation tun-

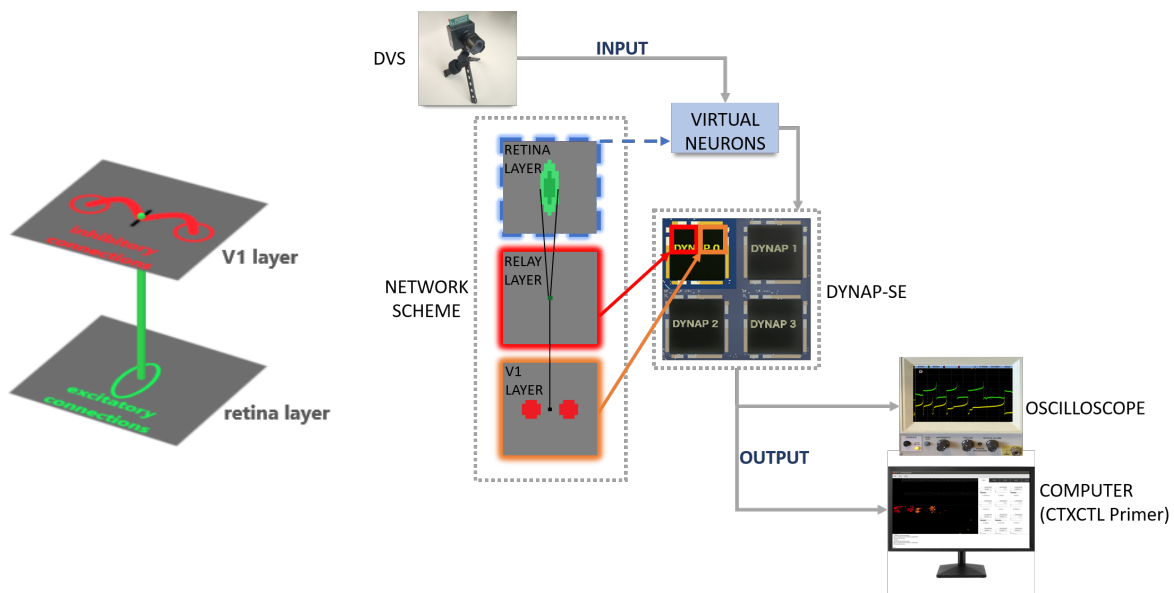


Figure 1: General structure of the network and connectivity scheme. (Left) The target neuron, indicated as a black bar on the V1 layer, receives feed-forward excitation from neurons of the retina layer within an elongated region, and recurrent inhibition from V1 neurons located in two circular clusters displaced symmetrically along the orientation selectivity bias provided by feed-forward afferent connections. The direction of the bar indicates the orientation to which the neuron will be eventually sensitive according to such connectivity scheme. The same pattern of connections is repeated for every neuron of the V1 layer. (Right) The overall system setup detailing how the model network has been physically mapped on the DYNAP-SE board. The DVS output is reproduced by a population of spiking ‘virtual neurons’ that acts as spike generator for the physical silicon neurons on the DYNAP-SE chips. The board can be connected to an oscilloscope, to observe the ‘membrane voltage’ of selected silicon neurons, and to a computer, through the CTXCTL Primer interface, to monitor the spiking activity of the four chips in real time. For more details see text.

ing curves of the neurons of interest in the V1 layer, offering a way to verify the efficacy of the recurrent clustered inhibition in molding the neurons’ tuning on specific values of these features. Moreover, the simulation process allowed us to verify the assumption of linearity of the network’s behaviour and to tune the significant parameters of the connectivity scheme, i.e. distance between the recurrent Gaussian clusters, size of the clusters and strength of the inhibition to obtain the narrowest tuning curves. For the sake of simplicity, the size of the feed-forward kernel and the strength of the excitation are kept constant.

This process leads to RFs for the neurons of the V1 layer that can be considered feature extractors for orientation and spatial frequency. The preferred orientation selectivity can be controlled by rotating the connectivity scheme, while the peak spatial frequency can be varied by scaling the displacement of the inhibitory kernels with respect to their size. However, due to the network structure through which they were created, they all have an even symmetry, i.e. they all exhibit the same (zero) phase. To overcome this limitation and obtain feature extractors with arbitrary phase values, we adopted a method similar to the one described in (Raffo et al., 1998). Considering

the one-dimensional projections of the spatial profiles of the RFs, obtained as the Fourier transform of their spatial frequency tuning curves, they can be summed in a convenient way to obtain a profile with the desired phase value. In particular, we considered 3 neurons of the V1 layer, the central one in position  $n$  and the lateral ones at the positions  $n - k$  and  $n + k$ , where  $k$  is chosen to be approximately the distance  $d$ , in terms of neuron index, between a target neuron of the V1 layer and the centers of the Gaussian clusters from which it receives recursive inhibition. This way, the maximum of the spatial profiles of the RFs of the lateral neurons will lay in correspondence with the minima of the spatial profile of the RF of the central neuron. By weighting the sum of the three profiles with  $\alpha = -\sin \psi - 0.5 \cdot \cos \psi$ ,  $\beta = \cos \psi$ ,  $\gamma = \sin \psi - 0.5 \cdot \cos \psi$  we can obtain a spatial profile with any desired phase value ( $\psi$ ).

### 2.3 Network Implementation on the DYNAP-SE Board

Based on the results obtained through simulations, we implemented the network on the DYNAP-SE board. It is worth noting that, to overcome the restrictions

posed by the chip, the network structure had to be modified. In particular, since every neuron can have at most 64 afferent connections, it was necessary an extra layer of neurons, the *relay layer*, between the retina layer and the V1 layer, to increase the number of available synapses. The relay layer receives excitation from the feed-forward kernels on the retina layer and projects one-to-one connections to the V1 layer, where the inhibitory recursion is then applied. The weights were adjusted so that the network with this new structure behaves in an equivalent way to the simulated one. Moreover, each chip is divided into four cores, and all the neurons belonging to a core share the same biases, including the synaptic weights of the afferent connections. Also, only two types of excitatory synapses and one type of inhibitory synapses were available for each neuron. Due to these constraints, the weights of the connections that form the kernels could not be assigned by sampling Gaussian functions. Instead, we adopted a constant value for the weights of the recurrent inhibitory connections, and two values for feed-forward excitatory connections (higher at the center and lower at the periphery of the kernel).

The DYNAP-SE board was interfaced with the computer through the software CTXCTL Primer, which provides a Python console that can be used to send commands to define the connectivity of the silicon neurons, to set biases to specific values, to send inputs to the neurons, and to record their activity.

## 2.4 Visual Stimuli Dataset

We choose as input sinusoidal gratings, widely used in the literature to investigate the response of cells in the primary visual cortex. Gratings with different orientations and spatial frequencies allow us to obtain the tuning curves that characterize a neuron's behavior. Specifically, the open source platform for behavioral science experiments PsychoPy (Peirce et al., 2019), was used to generate moving sinusoidal gratings with specific orientation, measured in degrees, spatial frequency, measured in cycles/deg, and temporal frequency, measured in Hertz. The moving gratings were displayed on a screen and recorded by the DVS. jAER (Delbruck, 2007), an open-source Java-based framework, was used to set the camera biases and record the data. Figure 2 shows how the sinusoidal grating is perceived by the DVS sensor. Since the DVS is sensitive to local contrast changes, bands of ON and OFF events are generated where the sinusoidal profile is steep enough. Conversely, where the profile is almost flat, contrast differences are too small to be detected by the sensor and no events are

generated, resulting in bands without events, which are wider or narrower according to the contrast sensitivity threshold. The spatial frequency information is preserved anyway, encoded in the period of the bands of events, not in their width; it is worth noting that the phase is shifted by  $90^\circ$ .

For a given distance  $D$  between the display and the DVS, the angular and the linear field of views of the sensor, AFOV and LFOV, respectively, can be expressed as a function of the focal length  $f$  of the lens and the size  $W$  of the pixel array:

$$\text{AFOV} = 2 \arctan \left( \frac{W}{2f} \right)$$

$$\text{LFOV} = \frac{W}{f} D$$

For the DVS128,  $W$  is  $128 \text{ pixels} \times 40 \mu\text{m/pixel} = 5.12 \text{ mm}$ .

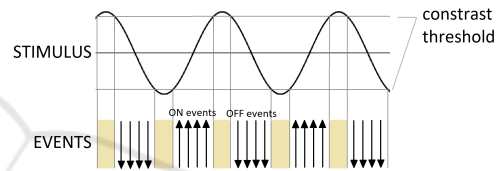


Figure 2: How the sinusoidal grating is converted in events by the DVS. Upward arrows represent ON events and downward arrows represent OFF events. Beige stripes are regions without events.

## 3 RESULTS

### 3.1 Linearity Test and Feature Tuning Characterization

First, we tested the linearity assumption. If the network behaves in a linear way, the firing rate of the neuron of interest should be modulated by the same temporal frequency of the grating used as input. Figure 3 shows that this condition is fulfilled for a wide range of temporal and spatial frequencies of the stimulus, both when the inhibitory recursion is turned off and when it is applied.

The simulations showed that recurrent clustered inhibition does indeed elicit the tuning of the neurons in the V1 layer on specific values of orientation and spatial frequency. The best results, i.e., the narrowest tuning curves, are obtained when the size of the recurrent inhibitory clusters and their distance from the target neuron are both comparable to the width of the feed-forward excitatory kernel.

Moreover, using recurrent clustered inhibition gives rise to well-structured Gabor-like RFs with a substantially lower number of synaptic connections than that

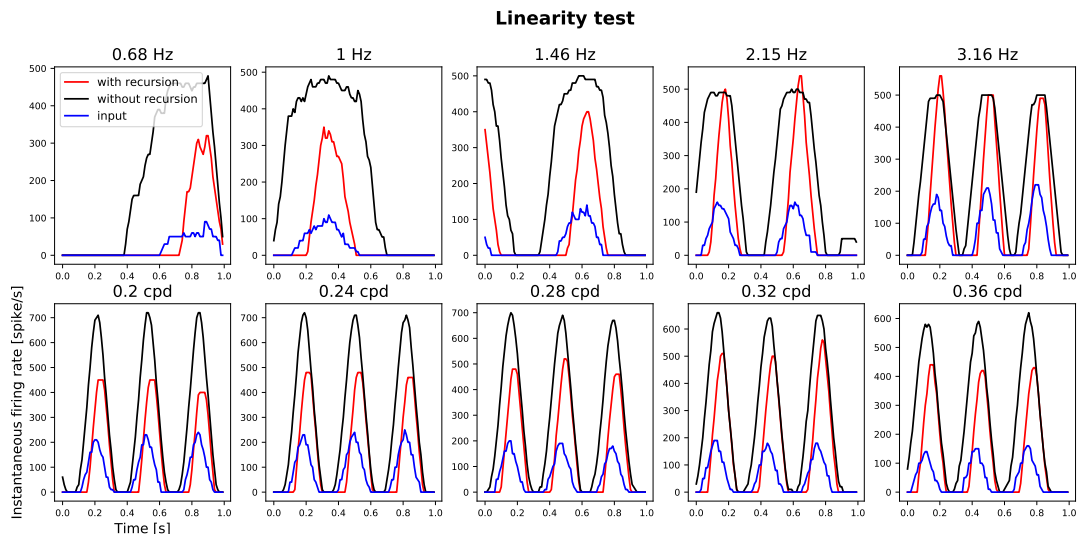


Figure 3: Instantaneous firing rate oscillations during 1s simulation. Black and red curves refer to the central neuron of V1 layer and the blue curve to four sample corresponding afferent neurons of the retina layer. In the first row the response to moving gratings with spatial frequency of 0.26 c/deg and temporal frequencies that vary as indicated; in the second row the response to moving gratings with temporal frequency of 3.16 Hz and spatial frequencies that are indicated.

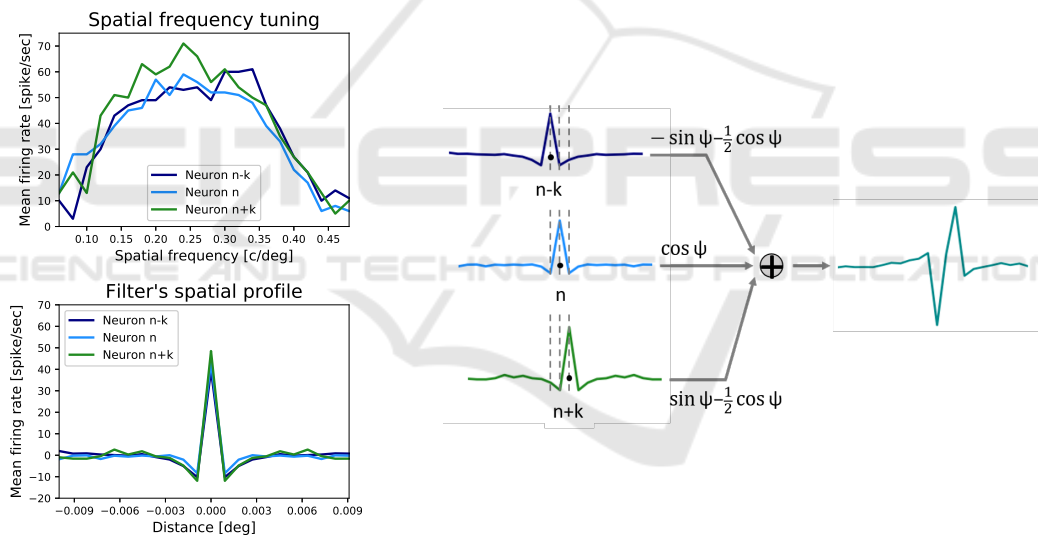


Figure 4: (Left) The spatial frequency tuning curves and their Fourier transforms for three sample neurons of the V1 layer (central neuron and two nearby neurons at distance  $d$  from it). The input grating used to obtain the curves had a temporal frequency of 3.16 Hz. (Right) The weighted sum of the spatial profiles to obtain a filter with an arbitrary phase value. The value of  $k$  can be chosen as being approximately equal to  $d$ .

required when using an exclusively feed-forward approach. To put this claim in numbers, we can consider a network in which both the feed-forward kernel and the recurrent clusters are 5 neurons wide. In this case, each neuron of the V1 layer receives 101 afferences. We can compare this result with equivalent networks in which the spatial profile of a V1 neuron's RF is obtained through exclusively feed-forward excitatory and inhibitory connections from the retina layer, defined by sampling a Gabor function whose

central lobe is 5 neurons wide. To obtain RFs with 3 and 5 subregions, 127 and 241 afferences to each neuron of the V1 layer are required, respectively. Besides, the orientation tuning curves of such neurons are comparable to the ones of the neurons of the recurrent network and the spatial frequency tuning curves are slightly worse.

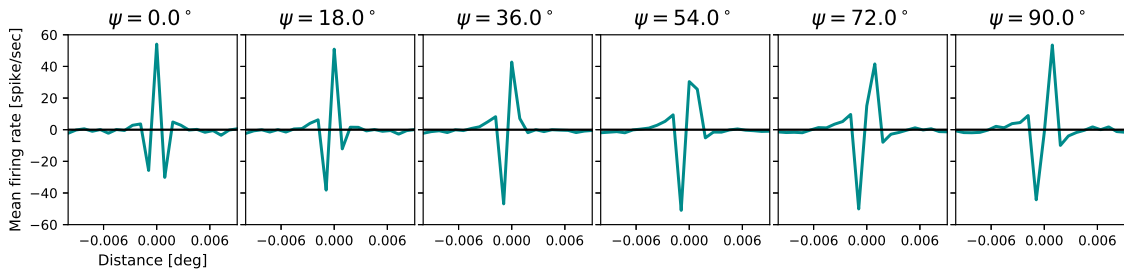


Figure 5: Filters with different phase values resulting from the weighted sum of responses of nearby neurons.

### 3.2 Spatial Profiles with Arbitrary Phase Values

As explained before, by linear weighting of neighboring RFs we can obtain higher-order RF profiles of any phase. For the sake of clarity, results are shown for the central 1D cross section of a neuron’s RF. The left side Fig. 4 shows the spatial frequency tuning curves and their Fourier transforms for three sample neurons, placed in central region of the V1 layer. We observe that the neurons are tuned to a specific spatial frequency value, and that the filters’ spatial profiles present a central positive lobe and two negative sidebands, resembling a Gabor function with even symmetry.

The right side of Fig. 4 shows how the weighted sum of the three RFs yields a resulting profile with a different phase value. Figure 5 showcases a series of resulting spatial profiles obtained with this approach for phase values ranging from 0° (corresponding to even symmetry) to 90° (corresponding to odd symmetry).

### 3.3 Functional Validation

The resulting bank of linear filters can be used as a minimal and controllable set of operators for extracting early vision features, directly from the spiking video stream provided by the DVS. Indeed, the spatial structure of the Gabor-like profiles allows us to aggregate ON and OFF temporal events according to local oriented band-pass spatial frequency channels, which are frequently used as front-ends of artificial vision systems (Dollr et al., 2014) (Luan et al., 2018). Although several tricks should be considered to efficiently implement a full multichannel representation, a flavour of the functionality of the proposed network is presented, for a single scale and four orientation channels. Figure 8 shows the results for a snapshot of a DVS recording featuring a moving hand; the panels show the activity of the DVS, the activity of the retina layer that reproduces ON events as spikes and the activity of the V1 layer for 4 different values of  $\theta$ . Brighter tones indicate higher firing rates. Only the neurons of the V1 layer whose orientation sensitivity

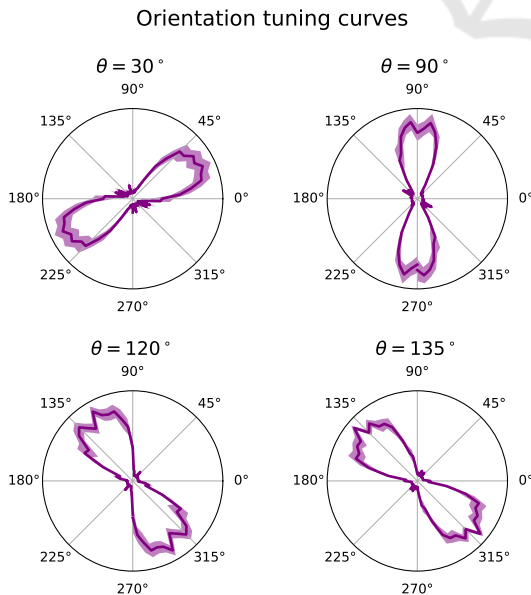


Figure 6: Examples of orientation tuning curves for different values of  $\theta$ . The input grating had a temporal frequency of 3.16 Hz.

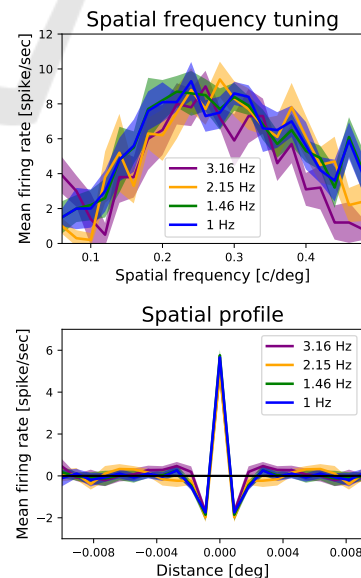


Figure 7: Spatial frequency tuning curves and their Fourier transforms for different temporal frequencies of the input grating.

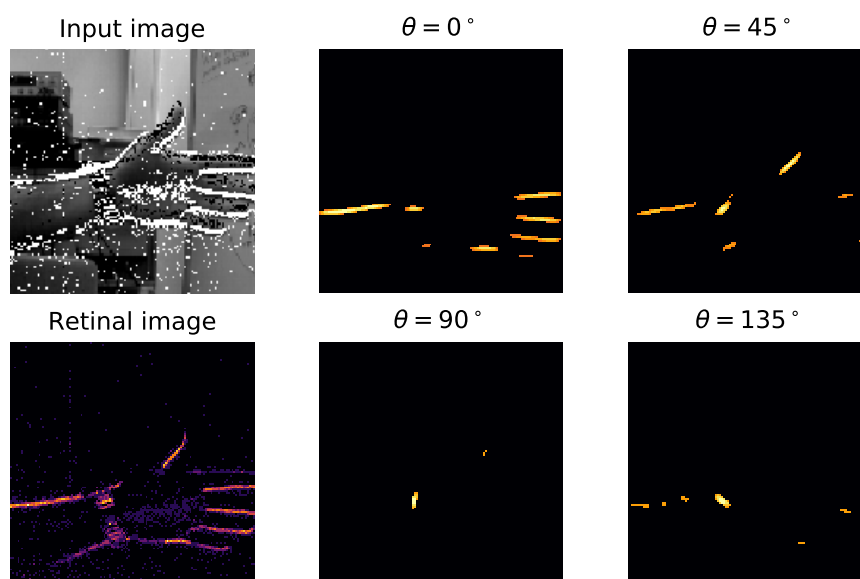


Figure 8: A snapshot of the activity of the DVS, the retina layer and the V1 layer with different preferred orientations for a real scene. The stream of events generated by the DVS is shown in the input image: 'ON' and 'OFF' events are represented as white and black squares overlaid to the corresponding scene acquired with a regular frame-based camera. Brighter tones indicate higher firing rates. For the sake of simplicity in the visualization, only the neurons of the V1 layer whose firing rates were over a certain threshold were represented. Cropped DVS240 recording from DVSFLOW16 dataset (Rueckauer and Delbruck, 2016).

matches the dominant orientation present in the image show a high firing rate.

### 3.4 Network Implementation on Chip

The DYNAP-SE board was programmed to implement the modified network structure we described previously. We used one of the 4 chips on the board, composed of 4 cores with 256 silicon neurons each. The chip is fabricated using a standard 0.18  $\mu\text{m}$  CMOS technology and the neurons and synapses biophysical behaviors are mimicked through parallel analog circuits (rather than time-multiplexed digital ones) which operate in sub-threshold regime to minimize the dynamic power consumption and to reproduce biologically plausible temporal dynamics. The computation is asynchronous and the memory elements (such as capacitors, CAM, and SRAM cells) are distributed across the computing modules, making the chip non Von Neumann. Despite the limitations posed by the hardware, the results in terms of tuning curves were comparable to the ones obtained in simulation. Since the behaviour of neurons and synapses on the DYNAP-SE board is not deterministic due to transistor mismatches, the curves were mediated over 10 sessions. Figure 6 shows the polar representation of the orientation tuning curves for four selected values of orientation. The spatial frequency tuning curves and their Fourier transforms are shown

in Fig. 7; different colors refer to different temporal frequencies of the gratings used as visual stimuli. It is worth noting that faster gratings elicit more events on the DVS and thus higher firing rate of the neurons on the retina layer, which then project to the relay layer and finally to the V1 layer. Nevertheless, the curves obtained for different temporal frequencies overlay: this is evidence of the fact that the emergence of ON and OFF subregions in the RF induced by recurrent inhibition successfully normalizes the firing rate in input.

## 4 CONCLUSIONS

Neuromorphic systems are a promising alternative to conventional von Neumann architectures in terms of power efficiency, computational flexibility, and robustness. Reproducing the dynamics of biological neurons, they represent ideal platforms to implement low-power bio-inspired devices. Here, we proposed an efficient way to implement spiking-based early-vision feature detectors on neuromorphic hardware. We took inspiration from the organization of the retinocortical pathway to obtain silicon neurons with Gabor-like RFs that are tuned to oriented visual stimuli with specific spatial frequency bandwidths. To achieve that goal while keeping the number of synaptic connections low, we successfully used recurrent



clustered inhibition, proving its efficacy in the context of discrete spiking neural networks. We also verified that the linearity assumption holds despite the high non-linearity of spiking neurons. Additionally, we showed how it is possible to combine such feature detectors to generate filters with arbitrary phase values, effectively implementing a full harmonic representation of the image signal. The harmonic signal description provided by the proposed neuromorphic circuit could be potentially used for a complete characterization of the 2D local structure of the visual signal in terms of the phase relationships from all the available oriented channels. This would pave the way to the implementation of complex bio-inspired networks for more demanding on-line visual tasks on neuromorphic hardware.

## ACKNOWLEDGEMENTS

This project has received funding from the European Research Council under the Grant Agreement No. 724295 (NeuroAgents).

## REFERENCES

- aiCTX (2018). <https://ai-ctx.gitlab.io/ctxctl/primer.html>. Last checked on Nov 20, 2019.
- Delbruck (2007). <https://github.com/SensorsINI/jaer>. Last checked on Nov 20, 2019.
- Dollr, P., Appel, R., Belongie, S., and Perona, P. (2014). Fast feature pyramids for object detection. *IEEE Transactions on Pattern Analysis and Machine Intelligence*, 36(8):1532–1545.
- Fleet, D. and Jepson, A. (1993). Stability of phase information. *IEEE Transactions on Pattern Analysis and Machine Intelligence*, 15(12):1253–1268.
- Jones, J. P. and Palmer, L. A. (1987). An evaluation of the two-dimensional Gabor filter model of simple receptive fields in cat striate cortex. *Journal of neurophysiology*, 58(6):1233–1258.
- Lichtsteiner, P., Posch, C., and Delbruck, T. (2008). A 128x128 120 db 15us latency asynchronous temporal contrast vision sensor. *IEEE journal of solid-state circuits*, 43(2):566–576.
- Luan, S., Chen, C., Zhang, B., Han, J., and Liu, J. (2018). Gabor convolutional networks. *IEEE Transactions on Image Processing*, 27(9):4357–4366.
- Milde, M., Renner, A., Krause, R., Whatley, A. M., Solinas, S., Zendrikov, D., Risi, N., Rasetto, M., Burelo, K., and Leite, V. R. C. (2018). teili: A toolbox for building and testing neural algorithms and computational primitives using spiking neurons. Unreleased software, INI, University of Zurich and ETH Zurich.
- Moradi, S., Qiao, N., Stefanini, F., and Indiveri, G. (2018). A scalable multicore architecture with heterogeneous memory structures for dynamic neuromorphic asynchronous processors (DYNAPs). *IEEE transactions on biomedical circuits and systems*, 12(1):106–122.
- Mügglér, E., Bartolozzi, C., and Scaramuzza, D. (2017). Fast event-based corner detection. In *Proceedings of the British Machine Vis. Conf. (BMVC)*, pages 1–11.
- Ogale, A. and Aloimonos, Y. (2007). A roadmap to the integration of early visual modules. *International Journal of Computer Vision*, 72:9–25.
- Osswald, M., Ieng, S., Benosman, R., and Indiveri, G. (2017). A spiking neural network model of 3d perception for event-based neuromorphic stereo vision systems. *Scientific Report*, 7:40703.
- Peirce, J., Gray, J. R., Simpson, S., MacAskill, M., Höchenberger, R., Sogo, H., Kastman, E., and Lindeløv, J. K. (2019). PsychoPy2: Experiments in behavior made easy. *Behavior Research Methods*, 51(1):195–203.
- Raffo, L., Sabatini, S. P., Bo, G. M., and Bisio, G. M. (1998). Analog VLSI circuits as physical structures for perception in early visual tasks. *IEEE Transactions on Neural Networks*, 9(6):1483–1494.
- Rueckauer, B. and Delbruck, T. (2016). Evaluation of event-based algorithms for optical flow with ground-truth from inertial measurement sensor. *Frontiers in neuroscience*, 10:176.
- Sabatini, S. P. (1996). Recurrent inhibition and clustered connectivity as a basis for Gabor-like receptive fields in the visual cortex. *Biological cybernetics*, 74(3):189–202.
- Sabatini, S. P., Gastaldi, G., Solari, F., Pauwels, K., Hulle, M. M. V., Diaz, J., Ros, E., Pugeault, N., and Krger, N. (2010). A compact harmonic code for early vision based on anisotropic frequency channels. *Computer Vision and Image Understanding*, 114(6):681 – 699.
- Stimberg, M., Brette, R., and Goodman, D. (2019). Brian 2: an intuitive and efficient neural simulator. *BioRxiv*, page 595710.